

# Electric-Field Assisted Growth and Self-Assembly of Intrinsic Silicon Nanowires

Ongi Englander,<sup>\*‡</sup> Dane Christensen,<sup>‡</sup> Jongbaeg Kim,<sup>‡</sup> Liwei Lin,<sup>‡</sup> and Stephen J. S. Morris<sup>†</sup>

*Department of Mechanical Engineering and Berkeley Sensor and Actuator Center, University of California, Berkeley, Berkeley, California 94720*

*Received January 18, 2005; Revised Manuscript Received February 8, 2005*

## ABSTRACT

Electric-field assisted growth and self-assembly of intrinsic silicon nanowires, in-situ, is demonstrated. The nanowires are seen to respond to the presence of a localized DC electric field set up between adjacent MEMS structures. The response is expressed in the form of improved nanowire order, alignment, and organization while transcending a gap. This process provides a simple yet reliable method for enhanced control over intrinsic one-dimensional nanostructure placement and handling.

Efficient and precise manipulation and placement of nanostructures at desired locations present key challenges toward the integration of nanostructures with larger scale systems. Techniques for directing one-dimensional nanostructure growth and improving nanostructure organization such as self-assembly could provide a profound impact to the ease of manufacturability of nanostructure-based systems and devices. Previously, one-dimensional nanostructures such as carbon nanotubes (CNTs) have been shown to respond to the presence of a DC electric field during synthesis to yield a better organized growth pattern, as nanotubes follow electric field lines.<sup>1–3</sup> This behavior is attributed to the strong polarizability of these one-dimensional nanostructures<sup>4</sup> and the electrophoretic effect. More specifically, the interaction mechanism is based on torque created on a CNT polarized by the electric field, which results in CNT growth along electric field lines. The torque is shown to be directly proportional to the applied electric field strength squared.<sup>1,2</sup> This approach permits the alignment of CNTs during their synthesis process. The post-synthesis control and placement of CNTs and metallic nanowires using DC, AC, and composite electric fields, in solution, have also been demonstrated.<sup>5–9</sup> In these experiments both ends of the nanostructure are free to interact with the field, and dielectrophoretic interactions play a significant role. The CNT response to purely DC fields, in these cases, is reported to be rather minimal.<sup>7–9</sup> This process, however, is not compatible with in-situ-growth alignment needs and is limited due

to the strong dependence on the evaporation time of the liquid solution. It is reasonable to conclude that a conductive one-dimensional nanostructure is required to realize a response to an electric field, and as such these methods are not compatible with insulators, for example. The response of semiconducting CNTs, however, has been documented for CNTs over a minimum length.<sup>1,10</sup> In ref 1, Joselevich and Lieber further suggest that, although the polarizability of metallic CNTs is approximately 3 times greater than that of a semiconducting CNT, if the CNT's energy of rotation, introduced by the electric field induced torque, is greater than its thermal excitation energy ( $kT$ ), a response to the presence of an electric field is possible. The energy of rotation is shown to be proportional to CNT's length.<sup>1</sup> Hence, longer nanostructures should show a more significant effect. Here we report on the observed response occurring during the synthesis of intrinsic silicon nanowires, in the presence of a locally applied DC electric field. Although, the charge carrier concentration in these nanowires is rather low, an appreciable improvement in nanowire organization is noted. This approach permits the localized growth and in-situ alignment of silicon nanowires to yield a two-terminal, self-assembled system.

As previously discussed,<sup>11</sup> we employ the resistive heating of a MEMS platform (growth structure) to locally initiate and sustain the vapor–liquid–solid (VLS) process for silicon nanowire (SiNW) synthesis. Silane (10% SiH<sub>4</sub> balance Ar), introduced at 100 sccm and 350 mTorr, is the vapor-phase reactant and gold–palladium (60%–40%) nanoparticles (formed upon the breakdown of a thin film layer) catalyze the reaction. The nanowires are strategically synthesized

\* Corresponding author. e-mail: ongi@me.berkeley.edu.

<sup>‡</sup> Department of Mechanical Engineering and Berkeley Sensor and Actuator Center.

<sup>†</sup> Department of Mechanical Engineering.

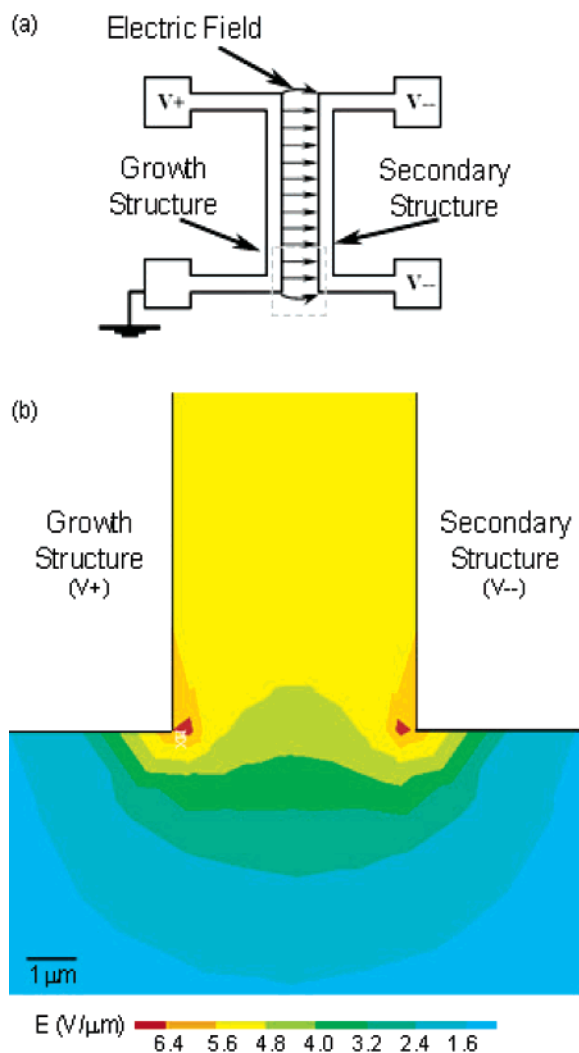


**Figure 1.** (a) Schematic top view of the experimental setup. The growth and secondary structures as well as the localized electric field between them are illustrated. (b) A plane encompassing the top surface of the MEMS structures from the 3D finite element simulation showing the electric field ( $\text{V}/\mu\text{m}$ ) strength between the two U-shaped structures near the corner portion as identified by a rectangular box in (a). The electric field intensification at the corners and fringe field effects are expected and evident in the simulation while the electric field at the central region away from the corners matches the calculated value of  $5.2 \text{ V}/\mu\text{m}$ .

using only silane as the vapor source, without the introduction of a dopant gas to the flow stream. As such, we ensure that synthesized nanowires are essentially electrically intrinsic. Synthesized SiNWs, typically 20 to 80 nm in diameter, grow at a rate of about  $1 \mu\text{m}/\text{min}$ . To study the response of the SiNWs to the presence of an electric field, a second MEMS structure (secondary structure) is positioned in close proximity to the growth structure's location, such that a local electric field may be exclusively set up between the two structures. The experimental setup is schematically depicted in Figure 1a. Overall, this approach allows for the localized synthesis of silicon nanowires to link together two MEMS structures and yield a self-assembled, two-terminal system. More specifically, highly doped, single-crystal silicon MEMS structures are positioned 5 to  $10 \mu\text{m}$  apart. A typical growth

structure is a  $5 \mu\text{m}$  wide, U-shaped structure with three sections measuring  $50 \mu\text{m}$ ,  $100 \mu\text{m}$ , and  $50 \mu\text{m}$ , respectively. The synthesis region is generally localized to the central region ( $100 \mu\text{m}$  portion) of the structure. The secondary MEMS structure may be identical to the first, or may alternatively take another shape. The dimensions and shape of the growth structure are important for controlling the location and extent of the SiNW growth,<sup>12</sup> while the secondary structure is required so that the local electric field may be attained. The use of an SOI (silicon on insulator) wafer for the MEMS structures' fabrication is suitable for fabricating suspended structures and further permits the isolation of MEMS structures from the substrate by locally removing the silicon substrate below the MEMS structures. Using thick MEMS structures,  $50 \mu\text{m}$  tall, and removing the substrate below them allows us to eliminate inhibiting effects resulting from nanowire interaction with the substrate during the synthesis process.<sup>3</sup>

The growth structure is actuated by placing one end at a driving voltage (typically 10 V) while the other end is grounded. Under these experimental conditions, a parabolic temperature distribution develops in the growth structure and the VLS process proceeds, locally, where the temperature requirement is met.<sup>11</sup> The local electric field is created by placing the secondary structure at a constant negative potential with respect to the growth structure, and thereby creating a voltage drop from the growth structure directed toward the secondary structure. The secondary structure, therefore, does not experience resistive heating effects. The secondary structure is connected to a power supply through a large resistance resistor (typically  $10 \text{ M}\Omega$ ) to prevent a significant voltage drop across the nanowires once a contact to the secondary structure is made. The magnitude of the voltage drop and the distance between the structures are used to approximate the strength of the electric field; however, finite element analysis was used to obtain improved estimates. In Figure 1b, a finite element model illustrates the electric field strength at the plane encompassing the top surfaces of the MEMS structures from a 3D model between the two U-shaped structures, near a corner. The potential difference of the growth structure (left) and the secondary structure (right) is set at 26 V, and the gap between the two structures is  $5 \mu\text{m}$ . The model illustrates fringe field effects, the intensification of the electric field strength at the corners, and a constant ( $5.2 \text{ V}/\mu\text{m}$ ) uniform electric field in the gap away from the corners.

Experimentally, the highest electric field strength that can be applied is limited by the dielectric breakdown value of the insulating oxide layer which separates the anchors of the MEMS structures from the substrate. Additionally, in all the experimental cases, the local horizontal electric field is slightly nonuniform due to the applied driving voltage drop across the growth structure. Electrophoresis, however, has been shown to take place regardless of homogeneity of the field.<sup>13</sup> In the example described above, the nonuniformity occurs since a linear voltage drop takes place along the growth structure, leading to a correspondingly linear decrease in the electric field strength. More specifically, the corner

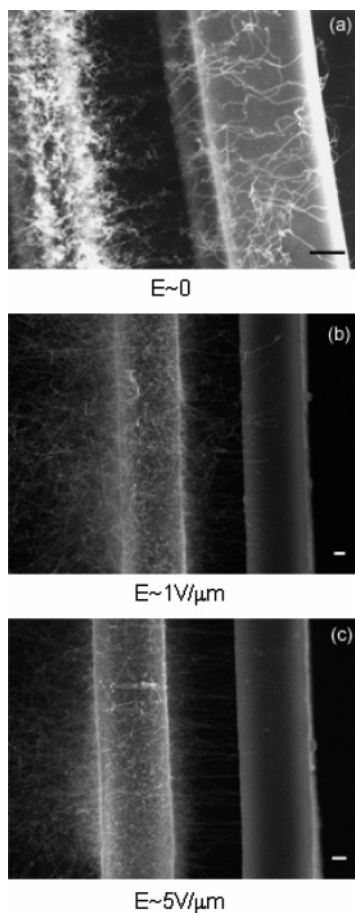


**Figure 2.** Illustration of silicon nanowire response to the presence of an electric field. In all cases the growth structure is on the left and the electric field is pointing from left to right. (a) No electric field applied, yielding poor organization across the gap. (b) Evidence of improved SiNW organization between the MEMS structures where a light electric field is present ( $E \sim 1 \text{ V}/\mu\text{m}$ ). (c) Further improvement in SiNW organization with increased electric field strength ( $E \sim 5 \text{ V}/\mu\text{m}$ ). A significant decrease in the number of nanowires growing over or resting on top of the secondary structure with increased electric field strength is noted. (All scale bars are  $1 \mu\text{m}$ .)

closest to the high-voltage end is subject to a slightly stronger electric field than the grounded end. Vertically, the electric field is uniform and perpendicular to MEMS structures.

Our results illustrate that, although the silicon nanowires are intrinsic, a response to the presence of the electric field is observable. The silicon nanowire synthesis process takes place at  $600\text{--}700^\circ\text{C}$  locally, and as such one would expect the presence of some free carriers. The following series of figures demonstrate experimentally that increased electric field strength leads to increasing nanowire order and organization. Figure 2a illustrates the lack of ordering and organization of the nanowire growth when no electric field is applied between the two structures across a  $5 \mu\text{m}$  gap. It is also observed that many nanowires are resting on the top surface of the secondary structure without making contact. In Figure 2b a weak electric field,  $1 \text{ V}/\mu\text{m}$  in strength, is applied between the structures and an improved level of nanowire ordering is visible across the  $5 \mu\text{m}$  gap. Figure 2c shows further improved nanowire ordering and alignment

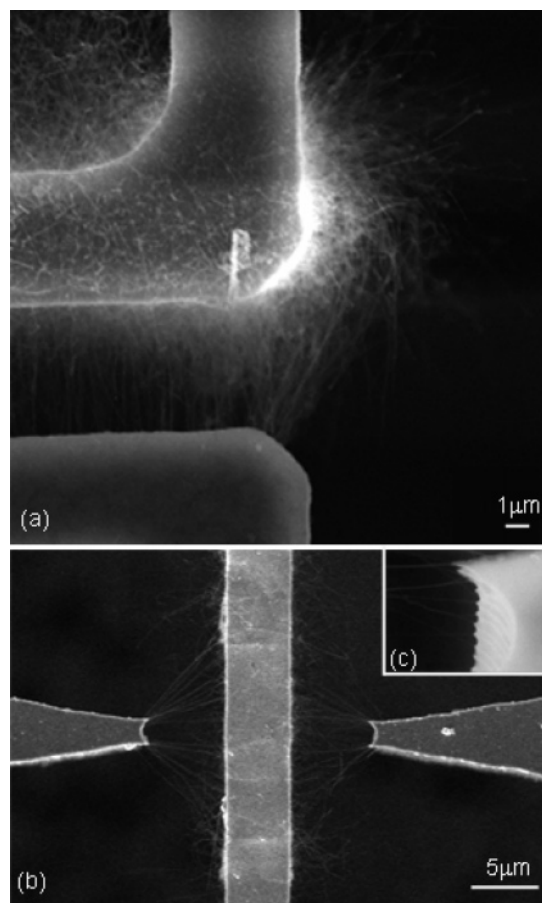


**Figure 3.** (a) SiNWs bending along fringe field lines as simulated in Figure 1b. The electric field strength at the corners is  $6.4 \text{ V}/\mu\text{m}$ , while the fringe field strength is  $\sim 3.8\text{--}4.1 \text{ V}/\mu\text{m}$  within  $1\text{--}2 \mu\text{m}$  to the right fringing area of the structures. (b) SiNW response to an electric field in the vicinity of a sharp tip. The growth structure is the center structure, while double-tipped secondary structures are positioned  $5 \mu\text{m}$  away. Significantly improved nanowire organization is observed as the electric field strength amplifies to  $\sim 25 \text{ V}/\mu\text{m}$  at the apex of the secondary structure. (c) Close up view of the bottom tip region of the left secondary structure. SiNW tendency away from the center (lower electric field strength) of the secondary structure as well as contact at protruding locations are evident.

as the electric field strength is increased to  $5 \text{ V}/\mu\text{m}$ . A comparison of Figure 2b,c reveals an approximately 5-fold decrease in the number of nanowires growing over and/or resting on the top surface of the secondary structure as the electric field strength is increased from  $1 \text{ V}/\mu\text{m}$  to  $5 \text{ V}/\mu\text{m}$ . Instead, more nanowires now make contact to the sidewalls of the secondary structure without growing over and/or resting on the top surface.

Since the purpose of the secondary structure is to establish a local electric field, its shape and location with respect to the growth structure can be manipulated to introduce variations to the local electric field. For example, the role of the fringe field and field intensification is examined in Figure 3a for two standard U-shape structures with electric field simulated as illustrated in Figure 1b. Although the micromachining process results in a rounded corner in Figure 3a, the influence of the fringe field effect on the orientation of the growth of nanowires is observed as nanowires bend

along fringe field directions. While the experimental setup yields a  $5.2 \text{ V}/\mu\text{m}$  uniform field, in the gap, away from the corners, the electric field strength at the corner can reach  $6.4 \text{ V}/\mu\text{m}$ , as indicated by the simulation in Figure 1b. By comparing the simulation (Figure 1b) and experimental results (Figure 3a), we can better assess the role of the electric field. The simulated electric field intensification at the corner is observed, as nanowires, transcending the gap within  $1 \mu\text{m}$  to the corner, are angled toward the corner. The fringe field effect is clearly seen for nanowires longer than  $3 \mu\text{m}$  with locations within the region of electric field strength greater than  $2.4 \text{ V}/\mu\text{m}$ .

To better visualize the role of the electric field, a sharply tipped secondary structure, as depicted in Figure 3b, is used. The sharp tip (crescent shaped secondary structure, with two sharp corners) is placed to the left and to the right of the growth structure. The electric field is maximized at the apex which contributes to the localized intensification of the electric field. The analytical solution to this problem suggests that, at the limit of an infinitely sharp tip, the electric field strength is infinite.<sup>14</sup> Experimentally, the sharp secondary structures, placed at  $-60 \text{ V}$ , are located  $5 \mu\text{m}$  away from the growth structure which is at approximately  $5 \text{ V}$  at the center. Based on these experimental conditions, the finite element model indicates a local electric field, approximately  $25 \text{ V}/\mu\text{m}$  at its strongest point or about twice as large as the directly calculated value at  $13 \text{ V}/\mu\text{m}$ , without consideration of field enhancement effects. As seen in Figure 3b, the SiNW seek the sharp tips. The electric field intensification, however, occurs locally and quickly drops in value away from the apex.<sup>14</sup> This effect is clearly seen as the order and organization of the nanowires, in regions  $10\text{--}15 \mu\text{m}$  away from the center of the growth structure, significantly decrease. The electric field strength in these regions is reduced to approximately  $5 \text{ V}/\mu\text{m}$ . Based on the nanowire behavior it is concluded that stronger fields will contribute to better SiNW alignment. Improved alignment as a function of increasing SiNW length is also evident in these experiments. The temperature distribution through the growth structure yields various SiNW growth rates and as such SiNWs of various lengths.<sup>11</sup> As predicted<sup>1</sup> and illustrated in Figure 3b, longer intrinsic nanowires show better alignment than shorter nanowires. Short nanowires, extending  $2\text{--}3 \mu\text{m}$  into the gap as visible in Figure 3b, appear to stray from the direction of the induced field and assume random orientations.

Further observations can be made with respect to the nanowire attachment to the crescent shaped secondary structures. We note, for example, that all contacts are made to the regions of the sharp tips where the electric field is the highest. In addition, the scalloped MEMS structure sidewalls (an artifact of the reactive ion etching process), as seen in Figure 3c, also contribute to regions of slightly stronger electric field, and nanowire contacts seem to be made at these protruding locations. It is also observed that no two nanowires make contact to the exact location on the secondary

structure. It is hypothesized that once a contact is made the local electric charge is partially neutralized or modified, and as such the local electric field strength is slightly reduced. Finally, the interaction among nanowires and the secondary structure is important in assessing the quality of each contact. While a contact to the sidewall should indicate a weld-type bond,<sup>15</sup> nanowires resting on the top surface may suggest a van der Waals interaction at best.

To summarize, a technique for localized growth and alignment of intrinsic silicon nanowires to yield a self-assembled, two-terminal system has been demonstrated. This technique is a combination of top-down and bottom-up methods and allows for localized silicon nanowire synthesis and their in-situ alignment using a DC electric field. The SiNWs appear to interact with the applied field and seek to align with the local electric field. Enhanced control over SiNW alignment and organization is evident at higher field strengths. This integrated process, with its improved control over the SiNW location and organization, yields a simple yet reliable and reproducible fabrication method which could be extended to other semiconducting one-dimensional nanostructures.

**Acknowledgment.** The authors thank the UC Berkeley Microfabrication Lab for their support and Mr. Ron Wilson for assistance with the SEM work. O.E. is partially funded by a Nanotechnology Fellowship from the State of California.

## References

- (1) Joselevich, E.; Lieber, C. M. *Nano Lett.* **2002**, *2*, 1137–1141.
- (2) Zhang, Y. G.; Chang, A. L.; Cao, J.; Wang, Q.; Kim, W.; Li, Y. M.; Morris, N.; Yenilmez, E.; Kong, J.; Dai, H. J. *Appl. Phys. Lett.* **2001**, *79*, 3155–3157.
- (3) Ural, A.; Li, Y. M.; Dai, H. J. *Appl. Phys. Lett.* **2002**, *81*, 3464–3466.
- (4) Benedict, L. X.; Louie, S. G.; Cohen, M. L. *Phys. Rev. B* **1995**, *52*, 8541–8549.
- (5) Smith, P. A.; Nordquist, C. D.; Jackson, T. N.; Mayer, T. S.; Martin, B. R.; Mbindyo, J.; Mallouk, T. E. *Appl. Phys. Lett.* **2000**, *77*, 1399–1401.
- (6) Fan, D. L.; Zhu, F. Q.; Cammarata, R. C.; Chien, C. L. *Appl. Phys. Lett.* **2004**, *85*, 4175–4177.
- (7) Chung, J.; Lee, J. *Sens. Actuators, A* **2003**, *104*, 229–235.
- (8) Chung, J. Y.; Lee, K. H.; Lee, J. H.; Ruoff, R. S. *Langmuir* **2004**, *20*, 3011–3017.
- (9) Chen, Z.; Hu, W. C.; Guo, J.; Saito, K. *J. Vac. Sci. Technol., B* **2004**, *22*, 776–780.
- (10) Dittmer, S.; Svensson, J.; Campbell, E. E. B. *Curr. Appl. Phys.* **2004**, *4*, 595–598.
- (11) Englander, O.; Christensen, D.; Lin, L. *Appl. Phys. Lett.* **2003**, *82*, 4797–4799.
- (12) Englander, O.; Christensen, D.; Chiao, M.; Kim, J.; Lin, L. In TRANSDUCERS '03. 12th International Conference on Solid-State Sensors, Actuators and Microsystems, Boston, MA, June 8–12, 2003; IEEE International Solid-State Sensors and Actuators Conference: vol. 1, 186–189.
- (13) Pohl, H. A. *Dielectrophoresis*; Cambridge University Press: Cambridge, 1978.
- (14) Landau, L. D.; Lifshitz, E. M. *Electrodynamics of Continuous Media*; Pergamon Press: Oxford, 1960.
- (15) Islam, M. S.; Sharma, S.; Kamins, T. I.; Williams, R. S. *Nanotechnology* **2004**, *15*, L5–8.

NL050109A